JACS
JOURNAL OF THE AMERICAN CHEMICAL SOCIETY

ARTICLE

pubs.acs.org/JACS

Mechanism of the Conformational Change of the F_1-ATPase β Subunit Revealed by Free Energy Simulations

Yuko Ito, Tomotaka Oroguchi, and Mitsunori Ikeguchi*

Graduate School of Nanobioscience, Yokohama City University, 1-7-29, Suehiro-cho, Tsurumi-ku, Yokohama 230-0045, Japan

Supporting Information

ABSTRACT: F_1-ATPase is an ATP-driven rotary motor enzyme. The β subunit changes its conformation from an open to a closed form upon ATP binding. The motion in the β subunit is regarded as a major driving force for rotation of the central stalk. In this Article, we explore the conformational change of the β subunit using all-atom free energy simulations with explicit solvent and propose a detailed mechanism for the conformational change. The β subunit conformational change is accomplished roughly in two characteristic steps: changing of the hydrogen-bond network around ATP and the dynamic movement of the C-terminal domain via sliding of the B-helix. The details of the former step agree well with experimental data. In the latter step, sliding of the B-helix enhances the hydrophobic stabilization due to the exclusion of water molecules from the interface and improved packing in the hydrophobic core. This step contributes to a decrease in free energy, leading to the generation of torque in the F_1-ATPase upon ATP binding.

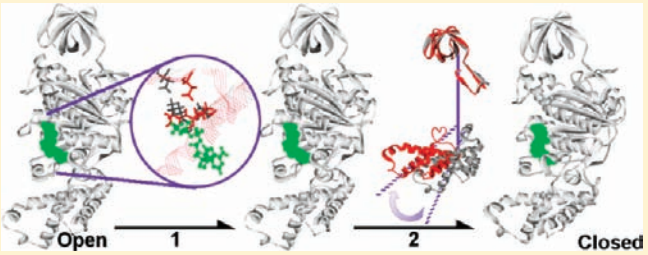

INTRODUCTION

F_oF_1-ATP synthase produces adenosine triphosphate (ATP), the high-energy compound used as biological energy for all living organisms.[1−10] F_oF_1-ATP synthase is a molecular rotary motor found in biological membranes. In mitochondrial F_oF_1-ATP synthase, the water-insoluble F_o moiety is embedded in the inner membrane and is composed of three subunits (a−c), whereas the water-soluble F_1 part of ATP synthase protrudes into the matrix space and is composed of five subunits ($\alpha-\varepsilon$). ATP synthesis/hydrolysis via rotation of the γ subunit in the F_1 moiety is coupled to an electrochemical diffusion gradient across F_o.[11]

Because the F_1 moiety (F_1-ATPase) is water-soluble and $\alpha_3\beta_3\gamma$ is the minimum catalytic unit for hydrolysis,[12,13] F_1-ATPase has been more extensively studied by crystallography and by single molecule experiments than the F_o moiety.[7,14−18] The three-dimensional structure of F_1-ATPase was determined for the first time in 1994.[19] The $\alpha_3\beta_3$ hexamer is arranged hexagonally around the central stalk, that is, the γ-subunit. Only the β subunits are catalytically active. The β subunits in the majority of crystal structures are in three different states: two closed (β_{DP} and β_{TP}) states and one open (β_E) state. Rotation of the γ subunit has been observed directly using single molecule fluorescent microscopy.[20,21]

ATP hydrolysis occurs in the β subunit with the 120° rotation of the γ subunit,[16,22] which can be divided into 80° and 40° substeps.[17,18] An 80° rotation in the γ subunit is induced by a conformational change from the open to the closed state in the β subunit upon ATP binding.[23] Upon structural transition from the open to closed form of the β_E subunit, its long α-helix-turn-α-helix pushes the bulge of the γ subunit, leading to stalk rotation.[24,25] Therefore, the structural transition of the β subunit via ATP binding is regarded as the major driving force for rotation of the γ-subunit. To elucidate the molecular mechanism of the "engine" of the molecular motor, the conformational change of the β subunit has been a tantalizing subject of study in F_1-ATPase.[26−29]

There have been experimental studies on the conformational change of the β subunit. Using NMR and mutagenesis, Yagi et al. elucidated that the switching of the hydrogen-bonding partner of Asp256 from Lys162 to Thr163 (the residue numbering is based on bovine mitochondrial F_1-ATPase) at the nucleotide-binding site and formation of the $\beta3/\beta7$ sheet are essential for the structural change from the open to closed state (Figure 1).[27] Furthermore, Masaike et al. identified hinge residues for the structural conversion.[28] We also studied the isolated β_E subunit by theoretical means, using molecular dynamics (MD) simulations. Even in the nucleotide-free state, principal component analysis (PCA) showed that motions in low-frequency modes were well correlated with the structural transition from the open to closed conformation, suggesting that flexibility in the direction of the structural transition is an intrinsic structural feature for the β_E subunit.[29] However, the observed flexibility was only at the backbone level. Moreover, the intensity of the fluctuation was insufficient to attain the fully closed conformation. As suggested by NMR, detailed conformational changes in both the main and the side chains (e.g., exchanges of hydrogen-bonding partners)

Received: August 5, 2010
Published: February 22, 2011

dx.doi.org/10.1021/ja1070152 | J. Am. Chem. Soc. 2011, 133, 3372–3380

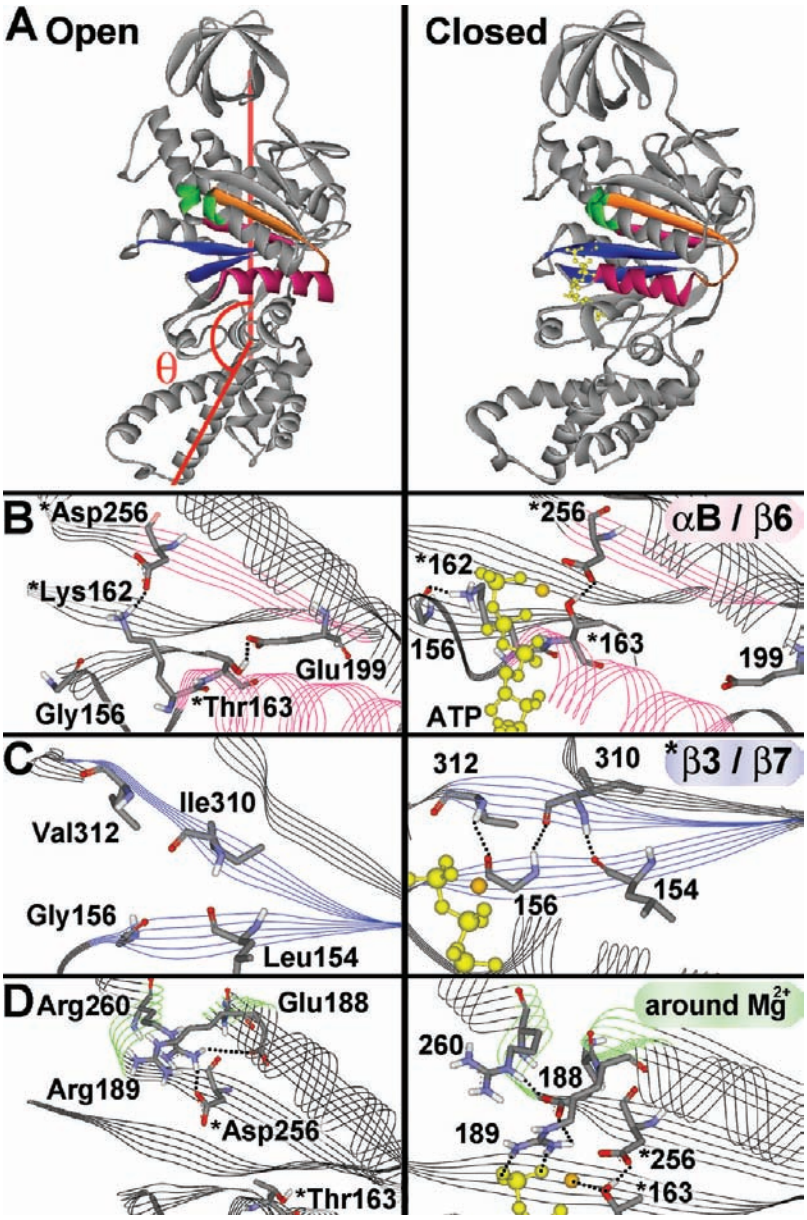

Figure 1. Isolated β subunits in the open (β_E) and closed states (β_{TP}) taken from a crystal structure (PDB code: 2JDI) (A). Angle θ represents the structural transition $\beta_E-\beta_{TP/DP}$. The definition of the angle measured between the axis connecting the center of mass of the N- and C-terminal domains and the axes of a helix (Glu399−Lys409) is taken from an NMR study.[26] Colored parts show key regions for the conformational change. Pink, blue, green, and orange indicate the αB-helix and β6 strand, the β3/β7 sheet, binding residues for the γ phosphate of ATP, and the β4 strand and hinge,[28] respectively. Enlarged views (B−D). "*" indicates essential residues for the open/closed conversion, identified by NMR.[27]

should be relevant to the entire mechanism of the structural conversion between the open and closed forms in the β subunit.

In terms of the temporal and spatial scale, such an open-closed conformational change is too broad to simulate directly using equilibrium all-atom MD simulations. Therefore, as an alternative method to bridge sampling between the open and closed states, we adopted a combination[30,31] of nudged elastic band (NEB)[32,33] and umbrella sampling MD simulations[34] to calculate the potential of mean force (PMF),[35] where the difference in root-mean-square deviation from the open (β_E) and closed states (β_{TP}) (ΔD_{rmsd}) of the β subunit is chosen as the reaction coordinate.[30,31,36,37] The PMF can provide the behavior of the system between the open and closed forms with free energy variation along the reaction coordinate. In this Article, we propose the entire mechanism of the conformational change in the β subunit. This information fills the gaps in the experimental data and provides a clue as to how the structural change associated with ATP binding contributes to the generation of torque.

METHODS

Computational Methods. A pair of free energy profiles for ATP-bound and -unbound states was calculated. We first generated two initial paths, with and without ATP, between the open and closed states of the monomeric β subunit using the NEB method[32,33] implemented in CHARMM.[38] The NEB method can be used to find a minimum energy path between two given reference structures. Subsequently, each

dx.doi.org/10.1021/ja1070152 |J. Am. Chem. Soc. 2011, 133, 3372–3380

configuration along the path undergoes umbrella sampling[34] MD simulations with restraints on the ΔD_{rmsd} order parameter. The ΔD_{rmsd} reaction coordinate has successfully provided functionally important information such as side-chain conformational changes that cause an overall structural transition.[30,31,36,37] Next, the free energy surface along the ΔD_{rmsd} order parameter from a series of the umbrella sampling simulations was calculated using a weighted histogram analysis method (WHAM).[39]

Reference Structures. In both paths with and without ATP, the E (β_E) and F chain (β_{TP}) subunits in the crystal structure (PDB code: 2JDI)[40] were used for the two end-points for the open and closed states, respectively. In the path with ATP, both the open and the closed structures bound to ATP were required as reference structures. Although the β_{TP} subunit could be used for the reference structure of the closed state, the crystal structure of the open β subunit with ATP is not available. Therefore, we modeled this structure using the following procedure. The β_{TP} subunit was superimposed onto the β_E subunit, where the fit was carried out over the C-terminal domain, and the coordinates of ATP bound in the β_{TP} subunit were transplanted into the β_E subunit. This process creates a model where the β_E subunit is bound to ATP in the adenine-binding pocket. Because an NMR study[27] has shown that mutant monomer β subunits can bind to nucleotide at the adenine-binding pocket even in the open conformation, the modeled structure is plausible as the reference structure for the open β subunit with ATP. In the path without ATP, the β_E and β_{TP} subunits were used as templates for the open and closed reference structures, respectively. For the closed structure, the ATP molecule was simply removed from the β_{TP} subunit.

Initial Path. Forty-one initial structures, including the end-point states, were generated via linear interpolation between the open and closed reference structures for each path (with and without ATP). This initial path was minimized using the steepest descent (SD) method. Subsequently, NEB by using the adopted basis Newton−Raphson (ABNR) minimization was used until convergence. The details for the SD and NEB method have been described by Arora et al.[30]

Umbrella Sampling Simulations. The 41 initial structures along the ATP-bound/-unbound paths were subjected to umbrella sampling MD simulations with the restraint w_j on the ΔD_{rmsd} order parameter.[36] $w_j = K_{rmsd}(\Delta D_{rmsd} - \Delta D_{min})^2$, where ΔD_{min} is the value around which ΔD_{rmsd} is restrained, and K_{rmsd} is a force constant. The ΔD_{rmsd} order parameter is the difference in the rmsd values of each intermediate structure from the reference open and closed states. It is given by the following: $\Delta D_{rmsd} = rmsd(X_t X_{open}) - rmsd(X_t X_{closed})$, where X_t is the instantaneous structure during the simulation, and X_{open} and X_{closed} are the two references, the open and closed isolated β subunits, respectively. Recently, ΔD_{rmsd} has been used as an order parameter successfully to characterize transition pathways between two structures in various proteins and DNA.[30,31,36,37] The advantage of using the ΔD_{rmsd} restraint is described by Banavali et al.[36] The 41 structures obtained from the NEB path optimization cover an rmsd range of 7.0 Å (the ΔD_{rmsd} value from −3.5 to 3.5 Å). The structures were separated by an interval of 0.2 Å in the ΔD_{rmsd} order parameter space. These 41 structures formed 41 windows for umbrella sampling runs.

In each window, the structure was solvated in a box of water and neutralized with counterions (Na^+ and Cl^-). The total number of atoms was 73 618 for the ATP-bound state and 72 399 for the ATP-free state, including 66 333 (bound) and 65 160 (unbound) atoms for the water molecules and 120 (bound) and 118 (unbound) atoms for the counterions. The initial distance between periodic images of the protein was 28.0 Å. After minimization of the initial structure in each window for 500 steps using SD, heating from 1 to 300 K was performed with harmonic constraints of 1.2 kcal/mol on the non-hydrogen atoms of the solute (total 3563 (bound) and 3531 (unbound) atoms) under NVT ensemble conditions. The system was then equilibrated for 100 ps with harmonic constraints of 1.0 kcal/mol on the non-hydrogen atoms under NPT ensemble (300 K and 1 atom) conditions. Subsequently, the rmsd force constant, K_{rmsd}, was gradually reduced from 3600 to 100 kcal/mol over a period of 0.5 ns in the NVT MD simulation. After equilibration, sampling simulations were performed for 1.0 ns, where the structures were simulated with a weak one-dimensional ΔD_{rmsd} restraint of 100 kcal/mol/Å^2 on the heavy atoms of the solute using NVT MD simulations.

All umbrella sampling simulations were carried out with the MD program MARBLE,[41] using CHARMM22/CMAP[42,43] for protein and TIP3[44] for water as force field parameters. Electrostatic calculations were performed using the particle mesh Ewald method with periodic boundary conditions.[45] The Lennard-Jones potential was truncated at 10 Å. In this study, the symplectic integrator for rigid bodies was used for constraints of the bond lengths and angles involving hydrogen atoms.[41] The time step used was 2.0 fs.

After all sampling simulations, the biased distribution along the reaction coordinate was checked. At a few points of the ΔD_{rmsd} reaction coordinate, the distribution overlap between adjacent windows was insufficient to explore the free energy surface; therefore, additional windows were appended. Those initial structures were generated via NEB using the neighbors.

Free Energy Calculation. The potential of mean force (PMF) along the ΔD_{rmsd} reaction coordinate was calculated by using WHAM[39] from a set of 1 ns umbrella sampling windows. The 2D free energy profiles along other additional parameters (e.g., the rmsd for a local structure, the distance between two atoms, and an angle between two domains) were obtained from the same trajectories of the 1D umbrella sampling without additional biased samplings. Even this level of the calculation can provide local structural behaviors (i.e., other parameters) along with the whole structural transition (i.e., the ΔD_{rmsd} reaction coordinate).[30,31,36,37]

RESULTS

The Conformational Change of the β Subunit with ATP. Figure 2A shows the free energy profile associated with the conformational transition pathway of the isolated β subunit with ATP along the ΔD_{rmsd} reaction coordinate. Shallow and deep free energy basins separated by an energy barrier exist in the open (ΔD_{rmsd} = −2.0 to −1.0 Å) and closed state (1.0−2.0 Å), respectively. This landscape indicates that ATP binding in the open β subunit is favorable to some extent, and the resulting intermediate, that is, the open β subunit bound to ATP, is transiently stable. The structural change from this intermediate to the closed state requires surmounting the energy barrier. Because the two minima (ΔD_{rmsd} = ∼ −2.0 and ∼ −1.0 Å) in the open state are separated only by a low energy barrier, they may not convincingly correspond to two different states. (Figure 2A). However, in this Article for convenience of the explanation of the structural change, the two minima are referred to as minima i and ii, respectively.

To obtain a more detailed mechanism of the conformational change for the ATP-bound pathway, the 2D free energy surfaces along the ΔD_{rmsd} order parameter with respect to various local structure changes were computed (Figure 3A−F). Regarding the 2D free energy maps of rmsd for various local structures, the rmsd values are calculated from the closed structure to show how the local conformations change toward the closed form along with the ΔD_{rmsd} order parameter. As well as the residues that have been identified as critical for ATPase activity and the subunit conformational change,[27,28] other residues were investigated comprehensively by monitoring their rmsd values and the

dx.doi.org/10.1021/ja1070152 |J. Am. Chem. Soc. 2011, 133, 3372–3380

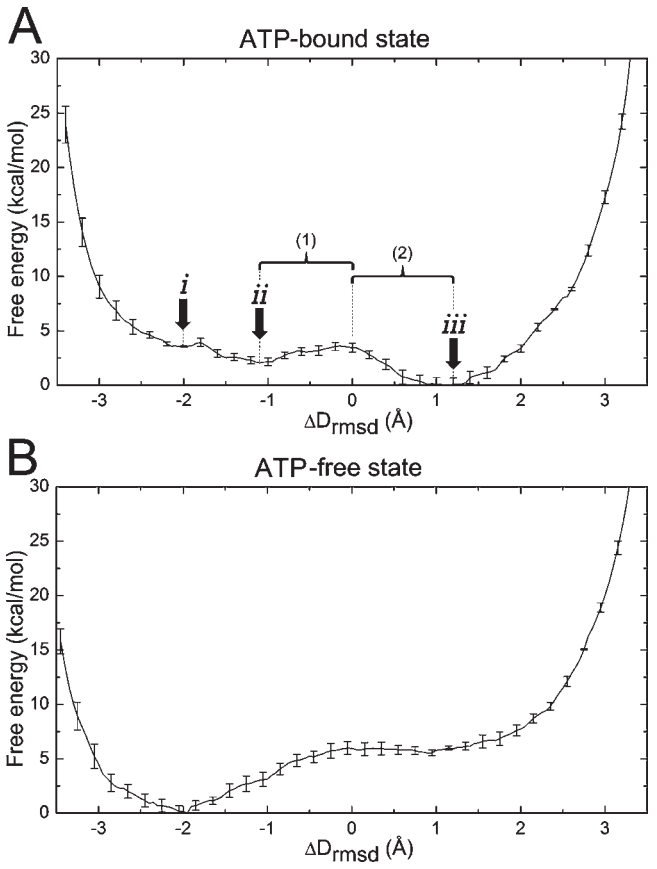

Figure 2. Free energy profiles associated with the conformational transitions of the isolated β subunit. The one-dimensional energy profile along the ΔD_{rmsd} reaction coordinate in the ATP-bound (A) and -unbound pathway (B). The error bars represent the standard error of the mean energy values determined from the trajectory divided into three phases. In the ATP-bound pathway (A), arrows indicate minima i, ii, and iii. The main barrier between minima ii and iii is divided into uphill (1) and downhill (2). The ΔD_{rmsd} value of the open (β_E) and closed forms (β_{TP}) in the 2JDI crystal structure is −3.92 and 3.92, respectively.

inter-residue distances. The results are classified along the ΔD_{rmsd} order parameter. The series of the mechanisms in this pathway are depicted in the order from the open to closed structure in Figure 4.

In the first stage of the stepwise conformational change (from the open state to minimum i in Figure 2A), the rmsd for the non-hydrogen atoms of Glu188, Arg189, the γ phosphate of ATP, and Mg^{2+} from the closed form in the crystal structure (β_{TP}) decreases rapidly at ΔD_{rmsd} = −2.5 to −2.0 Å (Figure 3A). Glu188 and Arg189 form a salt bridge and subsequently bind to the γ phosphate of ATP (Figure 4, open → i). Glu188 and Arg189 have been identified to contribute to the catalytic reaction.[27,46−50] Before these interactions are formed, the side chain of Arg189 is able to move without any restrictions, and Glu188 is coordinated by a salt bridge with Arg260 (Figure 4).

In the second stage corresponding to the 1D free energy profile from minimum i to ii, the hydrogen bond between the NHε/η proton of Arg260 and the Oδ atom of Asp256 is broken at ΔD_{rmsd} = −2.0 to −1.0 Å (Figure 3B). The strictly conserved residue Arg260 has been reported as an essential residue for the recognition of P_i (the cleaved γ phosphate).[51] Asp256 is a key residue in the Walker B motif conserved in many ATPases, and in the β subunit of F_1-ATPase, Asp256 has been reported to be essential for the conformational change induced by nucleotide binding.[27] Initially, Arg260 interacts with both Asp256 and Glu188 as described above. However, the new conformation of the Glu188 side chain due to its hydrogen bond with Arg189 and ATP in the former step (the open state → minimum i) intrudes into the space between Arg260 and Asp256, so that the salt bridge of Arg260 with Asp256 is broken (Figure 4, i → ii).

The third stage corresponds to a main barrier between minima ii and iii containing several processes. It is divided into two parts, uphill (1) and downhill (2), as shown in Figure 2A. Uphill (1) includes: (a) hinge flips (Φ, Gly178; Ψ, His177), (b) the $\beta3/\beta7$ sheet formation, and (c) Asp256 switching partners from Lys162 to Thr163. These structural changes appear to be coupled with one another, leading to a small loss of free energy.

(a) After the Asp256−Arg260 bond breaks, Arg260 still maintains the interaction with Glu188. Along with the elongation of the distance between the side chains of Asp256 and Arg260, the χ_2 dihedral angle of Arg260 is rotated toward the opposite direction to Glu188. This rotation drags the entire Glu188 residue toward the Arg260 direction (Supporting Information Figure S1A and B). Apparently, pulling Glu188 imposes a stress on the main chain of the Glu188 loop (Supporting Information Figure S2A−D). When this strain on the loop exceeds its elasticity, the backbone dihedral angles (Φ, Gly178; Ψ, His177) at the opposite side to the stressed loop are flipped (Figure 4 (a): ii → Int. and Supporting Information Figure S3A and B). The backbone dihedral angles (Φ, Gly178; Ψ, His177) have been reported as a hinge region for the closing motion, as illustrated by an orange coil in Figure 4.[28] The hinge flips (Φ, Gly178; Ψ, His177) shown here are equally observed in the path without ATP. Experimental evidence of the functional relevance of the hinge flips and the details of the hinge flips in the path without ATP are described in the section The Conformational Change of the β Subunit without ATP .

(b) When the $\beta3$ and $\beta7$ strands get close enough to interact with each other due to the Glu188 position shift (the details are described in Supporting Information Figure S1A and B), the dihedral angles at the P-loop (Gly156 and Gly157) rotate to form a backbone hydrogen bond between Gly156 and Val312 (Supporting Information Figure S4A−D). Once this additional hydrogen bond between the $\beta3$ and $\beta7$ strands is established, the formation of the $\beta3/\beta7$ sheet is completed (Figure 1C and Figure 4, (b): ii → Int.). The NMR study has proven that this $\beta3/\beta7$ sheet formation is essential for the β subunit to become the closed form, because an obstruction of the $\beta3/\beta7$ sheet formation via the Y311P substitution abrogates the open/closed conversion for the overall structure.

(c) During the $\beta3/\beta7$ sheet formation, the change of the backbone dihedral angles Ψ at Gly156 and Φ at Gly157 results in the structural change of the P-loop backbone (Supporting Information Figure S5A). Along with the structural change of the P-loop backbone, the side chain of Lys162 relocates by rotating the χ_1 and χ_4 dihedral angles of Lys162 (Supporting Information Figure S5A, C, and D). This rotation of the alkyl side chain of Lys162 distances the NHζ atom of Lys162 from the Oδ atom of Asp256 (Supporting Information Figure S5B). This is

dx.doi.org/10.1021/ja1070152 |J. Am. Chem. Soc. 2011, 133, 3372–3380

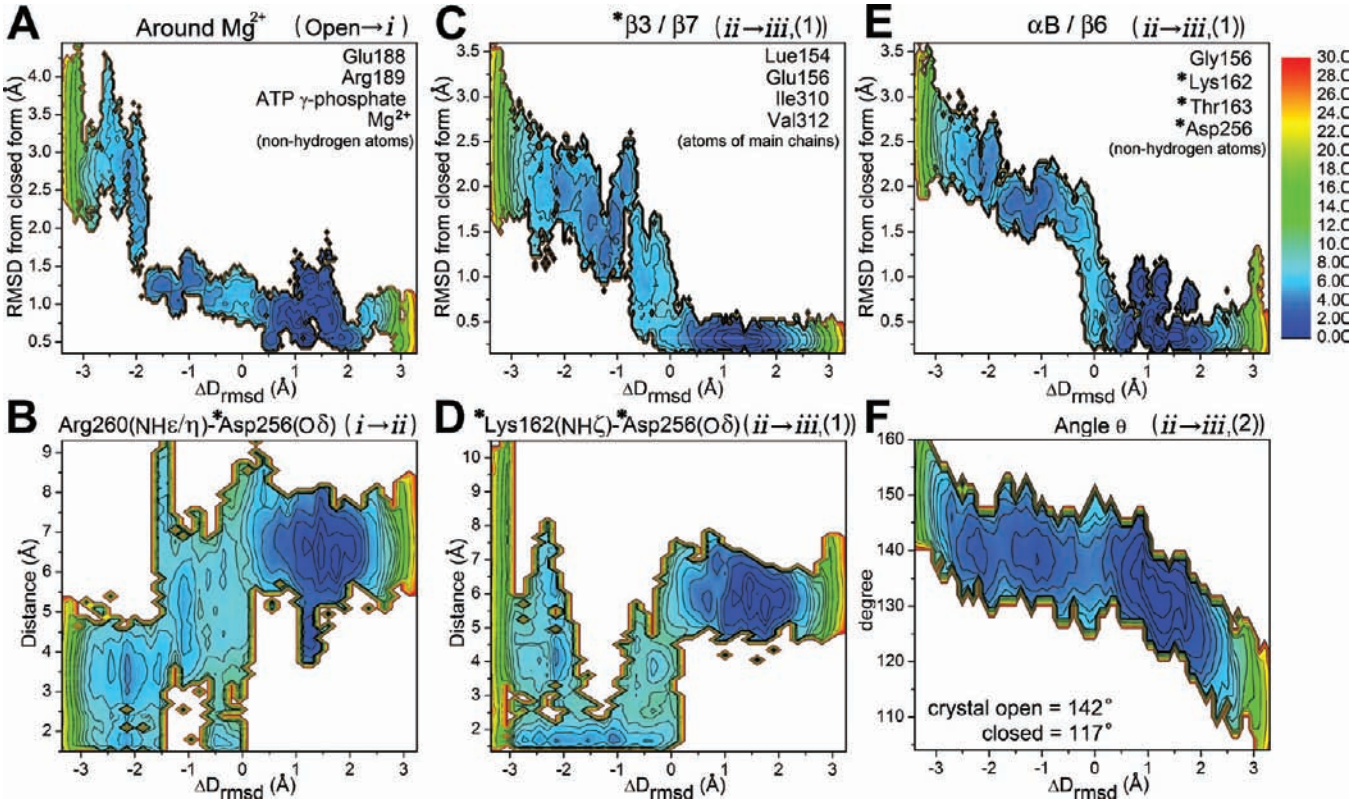

Figure 3. Local conformational changes associated with the structural transition of the β subunit in the ATP-bound pathway. Free energy surfaces along the ΔD_{rmsd} reaction coordinate (horizontal axis) and various variations (vertical axis); the rmsd of the side chains for residues around the γ phosphate from the closed form, β_{TP} (A), distance between the side chain of Arg260 and Asp256 (B), the rmsd of the main chain atoms for residues on the β3 and β7 strands from β_{TP} (C), distance between the side chain of Lys162 and Asp256 (D), the rmsd of the side chain for residues on the αB-helix and β6 strand from β_{TP} (E), and the angle θ (F). "*" indicates essential residues for the open/closed conversion, identified by NMR.[27]

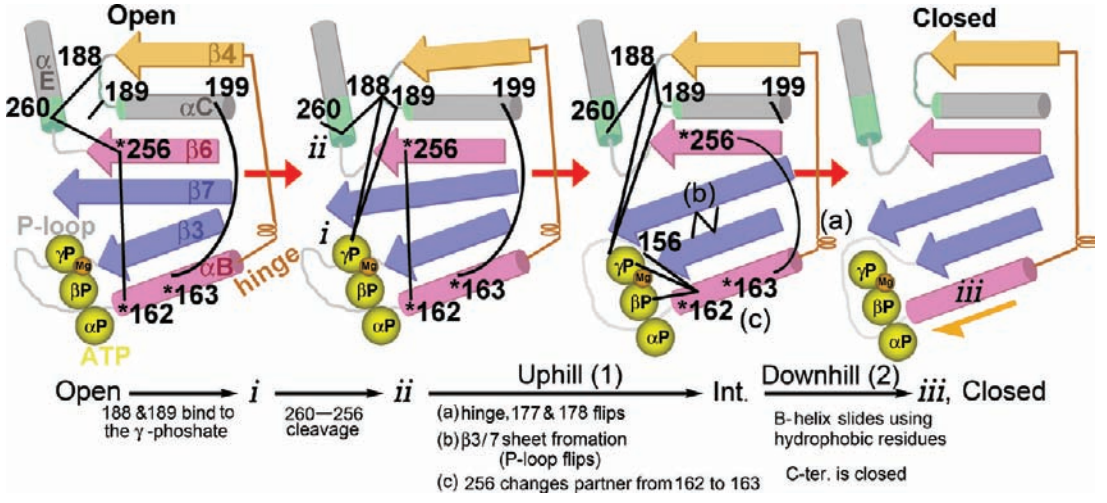

Figure 4. A schematic model for the conversion from the open to closed form of the β subunit. Color coding is the same as in Figure 1. "*" indicates essential residues for the open/closed conversion, identified by NMR.[27] Roman numerals correspond to the minima in Figure 2A. Int. represents the intermediate structure before downhill (2) starts.

the initiation of switching the hydrogen bond of Asp256 from Lys162 to Thr163 (Figure 3D,E, and Figure 4 (c): ii → Int.). Subsequently, the released side chain of Lys162 forms new hydrogen bonds with the backbone CO of Gly156 as well as the β and γ phosphates of ATP (Supporting Information Figure S6A and B). An NMR study has also proven that this hydrogen-bond switch is essential for the open/closed conversion of the entire β subunit structure because alanine mutants at Lys162, Thr163, and Asp256 are unable to attain the closed conformation even though they are capable of binding a nucleotide to the adenine binding pocket.[27]

dx.doi.org/10.1021/ja1070152 |J. Am. Chem. Soc. 2011, 133, 3372–3380

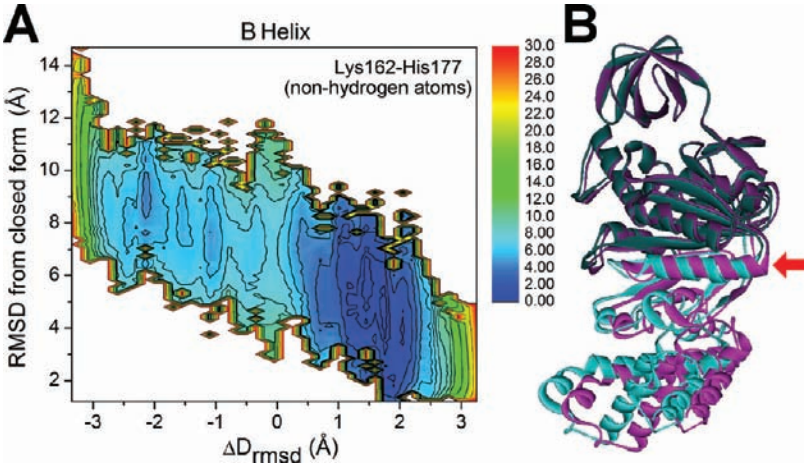

Figure 5. Free energy map for the rmsd of residues from Lys162 to His177 (non-hydrogen atoms), from the closed structure (β_{TP}), along the ΔD_{rmsd} reaction coordinate in the ATP-bound pathway (A). Superposition of the structure before and after the C-terminal domain movement, corresponding to the structure at ΔD_{rmsd} = 0.0 (magenta) and 1.4 Å (cyan), respectively. The fit is carried out over the N-terminal domain. The parts exhibiting a small structural change (i.e., residues 9−123 and 178−329) and a large change (i.e., residues 124−177 and 330−474) in a reaction coordinate from ΔD_{rmsd} = 0.0 to 1.4 Å are depicted with dark and light colors, respectively. The B-helix is marked by a red arrow.

After completion of the local conformational changes around the ATP binding site, the overall structural change, shown as the angle θ of the C-terminal domain[26] in Figure 1A, finally proceeds toward the closed form (Figures 3F and 4, Int. → iii). This closing movement of the C-terminal domain corresponds to the entire downhill region (2) of the 1D free energy profile (Figure 2A). This most large-scale conformational change of the C-terminal domain is supposed to generate the most torque used for the motor rotation. To identify the driving force for the movement of the C-terminal domain corresponding to the torque-generation step, we further investigated local structural changes at the downhill (2) phase. We found that the non-hydrogen atoms on the B-helix alter concertedly with movement of the C-terminal domain (Figure 5A). Figure 5B shows the superposition of the structures before and after movement of the C-terminal domain. It is clear that only the region below the B-helix, illustrated with the vivid color, moves relative to the upper portion of the nucleotide domain. The lower half of the β-subunit (magenta and cyan structures in Figure 5B) is shifted for one turn of the B-helix. This B-helix displacement stems from an alteration of the hydrophobic interactions on the B-helix. The B-helix contains not only the hydrophilic (Lys162 and Thr163)[27] and hinge residues (His177−Gly179)[28] described above but also many hydrophobic residues (Supporting Information Figure S7). Furthermore, residues on the upper portion facing the B-helix that make up the β4−7 sheets and C-helix are also mostly hydrophobic. Accordingly, the B-helix slides using its hydrophobic residues on the other hydrophobic surface, which appears to alleviate structural strains induced from the previous changes. Detailed information of the B-helix sliding (such as the changes in distances of the hydrophobic interactions between the B-helix and the other helixes/sheets) is provided in Supporting Information Figure S7. This B-helix displacement results in the conformational change of the entire C-terminal domain. The resulting structure at the minimum iii is more stable than the structure at the top of the peak by 4.0 kcal/mol, as shown in Figure 2A.

Analyzing this stabilization of the closed state, we found that there is a difference in the packing arrangements of the hydrophobic interface before and after the B-helix slide. Before completion of the B-helix displacement, the undulating hydrophobic surfaces are not tightly packed, and the interspace is loose enough to accommodate water molecules (Figure 6B). The cavity occupied by water molecules is constituted by the following hydrophobic groups: the side chain of Phe183 and Leu196, the alkyl part of Glu192, and the γ-methyl group of Thr163 (Supporting Information Figure S8). As the structure reaches the closed form, the interface packing is improved, and the number of the water molecules is decreased concomitantly with shrinking of the cavity (Figure 6A). Eventually, at minimum iii, there is little space between the hydrophobic interfaces for even a single water molecule to occupy (Figure 6C). Generally, water molecules inside hydrophobic surroundings prevent the formation of hydrophobic interactions. Therefore, after the water molecules are excluded, the hydrophobic moieties of those side chains make contacts and form the lowest free energy configuration.

NMR studies have reported that there are two closed forms for the β subunit; closed form I has a 25° angle θ difference between the open and closed states, while closed form II has a 35° difference.[26,52] Closed form I is observed in the F_1-ATPase complex, and closed form II is found in the monomer β subunit. Because we used the β_{TP} subunit of the F_1-ATPase complex, that is, closed form I for the end point structure, the path described here is the β subunit structural change between the open (β_E) and closed (β_{TP}) subunits. Therefore, structures that have an angle slightly less than closed form I (117°) are obtained at minimum iii (Figure 3F).

The Conformational Change of the β Subunit without ATP. Figure 2B shows the free energy profile associated with the conformational transition pathway of the β subunit without ATP along a one-dimensional reaction coordinate. There is a free energy basin in the open state (ΔD_{rmsd} = −2.5 to −2.0 Å). The open state is more stable than the closed state (ΔD_{rmsd} = 0.8−1.2 Å) by 6.0 kcal/mol. This result indicates that the closed conformation is unfavorable without ATP and that the ATP-free β subunit would fluctuate only around the open form. To attain the fully closed conformation of the β subunit, ligand binding is required.

Comparison of the pathways with and without ATP reveals the role of ATP. Also, there is interest in how the open form of the β

dx.doi.org/10.1021/ja1070152 |J. Am. Chem. Soc. 2011, 133, 3372–3380

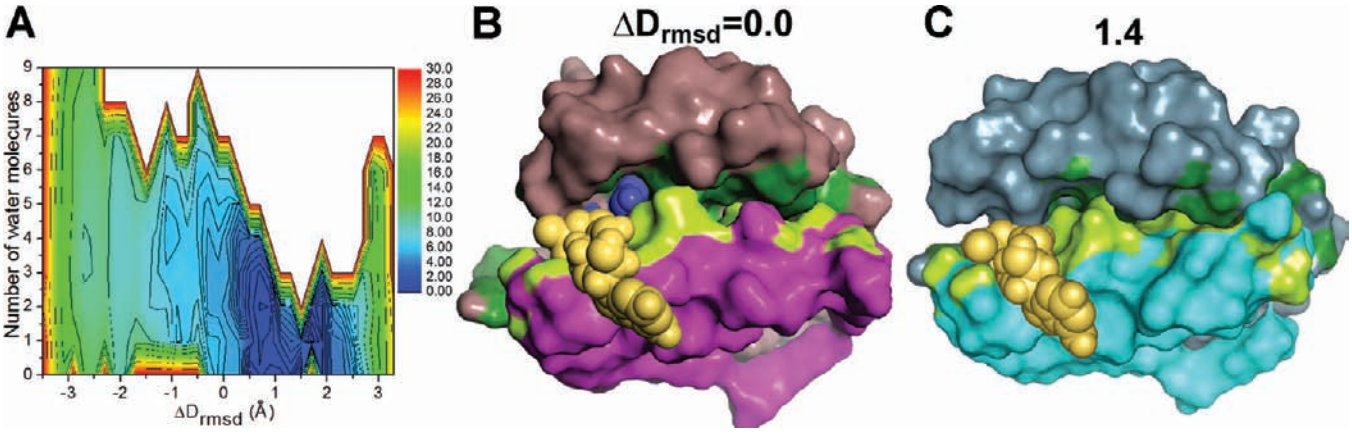

Figure 6. Free energy surface for the number of water molecules in the space formed by the hydrophobic surfaces of the B-helix and the other helices/sheets (i.e., the C-helix and β3−7 sheets) along the ΔD_{rmsd} reaction coordinate in the ATP-bound pathway (A). Snapshots of the packing of the hydrophobic surfaces at ΔD_{rmsd} = 0.0 (magenta) and 1.4 Å (cyan) are exhibited in (B) and (C), respectively. Hydrophobic parts of the interface are colored in green. The trapped water molecules in the interspace are indicated in blue. Color coding for dark/light is matched to Figure 5B.

subunit, without ATP, is stabilized. To identify these features, 2D free energy surfaces along the ΔD_{rmsd} order parameter with local structures are calculated. At ΔD_{rmsd} = −0.3 Å, the values of the dihedral angles Ψ and Φ (of the adjacent residues His177 and Gly178, respectively)[28] changed drastically (Supporting Information Figure S3C and D). As with the ATP-bound pathway, Arg260 and Glu188 play important roles for the hinge flip in the ATP-free pathway. Because there is no ATP molecule, the process of the hinge flip is much simpler than the ATP bound pathway. The side-chain rotation of Arg260 leads to the detachment of the NHε/η atom of Arg260 from the Oε atom of Glu188 and the Oδ atom of Asp256 at ΔD_{rmsd} = −0.3 Å, inducing the hinge flip (Supporting Information Figure S9). However, the dihedral angle rotations at the P-loop (Gly156 and Gly157) for the β3/β7 sheet formation are not observed, indicating that the ATP molecule manipulates the conformation of the P-loop during the structural change. The hinge flips occur at the last period before the overall structure change from the open to closed form (Supporting Information Figure S3E), indicating that the conformational changes at His177 and Gly178 trigger the entire structural change. In other words, these residues contribute to the stabilization of the open form structure. This result agrees with experimental data in which alanine mutations at positions 177 and 178 increase tendency of ADP inhibition, in which the closed form is possibly overstabilized relative to the open form. As shown in Supporting Information Figure S3D, Gly178 in the open form adopts a positive value for the Φ angle. However, the angles Ψ and Φ cannot adopt all possible values because of steric restrictions. Only glycine is able to adopt a positive value of Φ. The result of the Φ value at Gly178 explains why the G178A mutation leads to destabilization of the open form, resulting in stabilization of the closed form.

This type of flip rotation of the dihedral angles Ψ at residue i and Φ at i+1 is known as "peptide plane flipping", which is characterized by movement about the axes defined by the C_i^{α}−C_i^{o} and N_{i+1}^{H}−C_{i+1}^{α} (at this i+1 position, glycine is expected) bond vectors via low energy, resulting in conformational changes in proteins.[53−55] As described above, this hinge flipping is observed in the path with ATP as well. Consequently, the flipping of angle Ψ at His177 and angle Φ at Gly178 are intrinsic features of the β subunit for the open/closed conversion, regardless of whether ATP is bound or not.

DISCUSSION

Because the open/closed conformational change in the β subunit is responsible for the driving force of rotation of the γ subunit, insights into the residues involved in the structural change have been intriguing. As the result, several regions in charge of the structural change have been identified.[27,28] However, it is difficult to comprehend the entire picture of the consecutive conformational change via these discrete information. Here, we propose the pathway of the entire open/closed conversion for the β subunit with and without ATP for the first time. The details of the conformational change on the pathway agree with the experimental data.[27,28] Moreover, the maximum difference of the free energy between the peak of the main barrier and closed state in the 1D profile of the ATP-bound path represents the most large-scale movement of the β subunit (Figures 2A and 3F), suggesting that the theoretically obtained pathways are reasonable.

In our previous equilibrium MD simulation for the isolated β_E subunit, although a large fluctuation in the direction of the structural transition has been observed in low-frequency PCA modes, the intensity of the fluctuation was insufficient to attain the fully closed conformation.[29] This is confirmed by the free energy map of the projections of the structural transition onto the low-frequency PCA mode, observed in the previous equilibrium MD simulation for the nucleotide-free β subunit (Supporting Information Figure S10). Although the β subunit possesses an intrinsic flexibility of the direction of the structural transition, the β subunit without a nucleotide fluctuates only in the open state. The free energy profiles obtained in the current study indicate that ATP binding promotes the structural change from the open to closed form, while the open form is populated in the ATP-free state (Figure 2A and B). The 2D free energy surfaces with the rmsd from the open and closed forms for the ATP-bound and ATP-free states (Supporting Information Figures S11 and S12) show the structural properties more clearly. This is consistent with results of the NMR study; only nucleotide binding can induce the conformational change from the open to fully closed form.[26]

In the ATP-bound pathway, the entire conformational change is accomplished roughly in two characteristic steps: changing of the hydrogen bond network around ATP and the dynamic

C-terminal domain movement via sliding of the B-helix. These steps are mainly manipulated by polar and hydrophobic interactions, respectively. ATP is only directly involved in the former step. It is clear that the role of ATP binding primes the conformational change in the β subunit.

In the former step, the binding of negatively charged ATP perturbs the extensive network of polar residues in the core region, and the perturbed network is propagated progressively. According to the 1D energy profile, uphill (1), which is the hinge flips (Ψ177 and Φ178),[28] the $\beta3/\beta7$ sheet formation, and Asp256 switching hydrogen-bonding partners,[27] controls the rate of the inward transition. Glu188 and Arg260 have been identified as important residues for the ATP hydrolysis. In addition, the present study reveals that these residues play important roles in the hinge flips as well, where Arg260 controls the Glu188 position. In a mutant F_1-ATPase, $\alpha_3(\beta E188D)_3$ study,[56] at low ATP concentration the ATP-binding dwell becomes longer and the catalytic dwell disappears, which cannot be observed in the wild type. Moreover, in another mutant $\alpha_3\beta_2(\beta E188D)$ study, the temperature-sensitive reaction in the single mutant occurs at the ATP binding angle.[57] These results certainly indicate that Glu188 is deeply involved in the β subunit structural change with ATP binding. Presumably, in the βE188D mutant the shorter side chain at the 188 position has a different behavior for the interaction with Arg260 and cannot induce the Ψ177 and Φ178 flips[28] in the same way as the wild type.

The dihedral angle rotations of the P-loop (Ψ156 and Φ157) to form the $\beta3/\beta7$ sheet formation induce the side-chain rotation of Lys162, resulting in switching of the hydrogen bonds of Asp256 from Lys162 to Thr163. These conformational changes take place in line. The residues reside on the Walker A (Gly156, Lys162, and Thr163) and Walker B (Asp256) motifs, which are highly conserved in the Walker-type ATPase family and essential for ATP-binding and hydrolysis. The previous[27] and current studies suggest that these universal motifs also play a role in facilitating a conformational change in accordance with ATP binding in the family. Moreover, regarding the Walker A motif, which has the consensus sequence (GXXXXGKT/S), the first G and the second last K correspond to Gly156 and Lys162 in the β subunit. Their simultaneous conformational changes provide a new insight into the conserved sequence motif.

One of the most prominent features of the latter step is that the sliding of the B-helix enhances the hydrophobic stabilization to accumulate free energy for motor torque due to the exclusion of water molecules and the improved packing density of the hydrophobic interaction. In the light of its entropy loss, hydrophobic stabilization with exclusion of water is easy to conceive intuitively and, in fact, has often been postulated, such as in the process of the protein folding.[58−60] Moreover, the hydrophobic sliding in itself also appears to be advantageous to accumulate free energy. During the B-helix sliding via the change in the hydrophobic interaction, the hydrophilic residues Lys162 and Thr163 on the same B-helix maintain their important hydrogen bonds, which were made in the previous step. Such sliding of hydrophobic residues while maintaining the hydrogen bonds has been reported to facilitate large-scale conformational changes with a minimal energy penalty.[61]

In nature, the β subunit is employed as a component of the F_1-ATPase. According to experimental data, the dissociation constant (K_d) of nucleotides in the F_1-ATPase complex is much smaller than that in the monomer β subunit.[62] Therefore, when the α and γ subunits of F_1-ATPase are taken into account, in particular, the catalytically important residues αArg373 and αSer344, the free energy of the closed state in the ATP-bound pathway will probably be lower relative to the open state and the peak of the main barrier (Figure 2A). However, the residues participating in the conformational change of the β subunit (reported in this current study) are mostly orientated into the interior and not exposed to the adjacent subunits. Therefore, it seems unlikely that these regions are affected sterically and electrostatically when the β subunit is in the complex. Thus, the conformational change mechanism presented here will be the same in the complex.

In the F_1-ATPase complex, the conformational change of $\beta_E \rightarrow \beta_{TP}$ that occurs upon binding to ATP (simulated here) is coupled to $\beta_{HC} \rightarrow \beta_E$ upon ADP release during the 80° γ rotation in the 120° cycle,[17,18,63,64] where β_{HC} is the "half-closed" structure found in 2001.[65] The transition $\beta_E \rightarrow \beta_{TP}$ is the inward movement, whereas $\beta_{HC} \rightarrow \beta_E$ is the outward movement. The opposite structure movements are coupled. As shown in this study, the inward structural change yields energy. Although we did not calculate the free energy profile of the β subunit binding ADP+Pi or ADP, the outward movement with these nucleotides is probably endoergic. Therefore, the exoergic conformational change ($\beta_E \rightarrow \beta_{TP}$) will cover the endoergic energy loss of the outward movement ($\beta_{HC} \rightarrow \beta_E$). We assume that such energy compensation is a prime reason that the F_1-ATPase adopts the binding change mechanism.[22] In addition, when inhibited by Mg-ADP, the closed state of the β subunit is overstabilized and will therefore have a larger stabilization energy than the energy produced from the $\beta_E \rightarrow \beta_{TP}$ inward transition.[66]

Finally, our results show that ATP binding and the conformational change in the β subunit are tightly coupled. The advantage of the tight coupling for the motor engine would be that the γ rotation can be strictly regulated via the β subunit, which can change conformation only through nucleotide binding, thus avoiding unproductive rotations due to severe thermal fluctuations. Moreover, "reversibility" is one of the major distinctive features of this enzyme. Such a transition with a barrier is desirable to control the rotational direction of the motor for ATP hydrolysis/synthesis.

■ ASSOCIATED CONTENT

Supporting Information. Full author list for ref 42; snapshots of the structures and/or 2D energy surfaces of the ATP-bound pathway for various local structure changes (Figures S1, S2, S3A, B, S4−6, S10, S11); 2D energy surfaces of the ATP-free pathway for various local structure changes (Figures S3C−E, S9, S12); hydrophobic interactions and their distance information for the B-helix sliding (Figure S7); and snapshots of the structure around water molecules before and after the C-terminal domain movement (Figure S8). This material is available free of charge via the Internet at http://pubs.acs.org.

■ AUTHOR INFORMATION

Corresponding Author
ike@tsurumi.yokohama-cu.ac.jp

■ ACKNOWLEDGMENT

We thank Professor Shigehiko Hayashi (Kyoto University) for helpful discussions. This work was supported by Grants-in-Aid

for Scientific Research from the Ministry of Education, Culture, Sports, Science, and Technology of Japan (MEXT) and Research and Development of the Next-Generation Integrated Simulation of Living Matter, a part of the Development and Use of the Next-Generation Supercomputer Project of MEXT.

REFERENCES

(1) Futai, M.; Kanazawa, H. *Microbiol. Rev.* **1983**, *47*, 285–312.
(2) Futai, M.; Noumi, T.; Maeda, M. *Annu. Rev. Biochem.* **1989**, *58*, 111–136.
(3) Senior, A. E. *Annu. Rev. Biophys. Biophys. Chem.* **1990**, *19*, 7–41.
(4) Pedersen, P. L.; Amzel, L. M. *J. Biol. Chem.* **1993**, *268*, 9937–9940.
(5) Boyer, P. D. *Annu. Rev. Biochem.* **1997**, *66*, 717–749.
(6) Walker, J. E. *Angew. Chem., Int. Ed.* **1998**, *37*, 2308–2319.
(7) Weber, J.; Senior, A. E. *Biochim. Biophys. Acta* **2000**, *1458*, 300–309.
(8) Kinosita, K., Jr.; Yasuda, R.; Noji, H.; Ishiwata, S.; Yoshida, M. *Cell* **1998**, *93*, 21–24.
(9) Gao, Y. Q.; Yang, W.; Karplus, M. *Cell* **2005**, *123*, 195–205.
(10) Karplus, M.; Gao, Y. Q. *Curr. Opin. Struct. Biol.* **2004**, *14*, 250–259.
(11) Rastogi, V. K.; Girvin, M. E. *Nature* **1999**, *402*, 263–268.
(12) Futai, M. *Biochem. Biophys. Res. Commun.* **1977**, *79*, 1231–1237.
(13) Dunn, S. D.; Futai, M. *J. Biol. Chem.* **1980**, *255*, 113–118.
(14) Ren, H.; Allison, W. S. *Biochim. Biophys. Acta* **2000**, *1458*, 221–233.
(15) Cherepanov, D. A.; Junge, W. *Biophys. J.* **2001**, *81*, 1234–1244.
(16) Yasuda, R.; Noji, H.; Kinosita, K., Jr.; Yoshida, M. *Cell* **1998**, *93*, 1117–1124.
(17) Yasuda, R.; Noji, H.; Yoshida, M.; Kinosita, K., Jr.; Itoh, H. *Nature* **2001**, *410*, 898–904.
(18) Shimabukuro, K.; Yasuda, R.; Muneyuki, E.; Hara, K. Y.; Kinosita, K., Jr.; Yoshida, M. *Proc. Natl. Acad. Sci. U.S.A.* **2003**, *100*, 14731–14736.
(19) Abrahams, J. P.; Leslie, A. G.; Lutter, R.; Walker, J. E. *Nature* **1994**, *370*, 621–628.
(20) Noji, H.; Yasuda, R.; Yoshida, M.; Kinosita, K., Jr. *Nature* **1997**, *386*, 299–302.
(21) Itoh, H.; Takahashi, A.; Adachi, K.; Noji, H.; Yasuda, R.; Yoshida, M.; Kinosita, K., Jr. *Nature* **2004**, *427*, 465–468.
(22) Boyer, P. D. *Biochim. Biophys. Acta* **1993**, *1140*, 215–250.
(23) Adachi, K.; Oiwa, K.; Nishizaka, T.; Furuike, S.; Noji, H.; Itoh, H.; Yoshida, M.; Kinosita, K., Jr. *Cell* **2007**, *130*, 309–321.
(24) Furuike, S.; Hossain, M. D.; Maki, Y.; Adachi, K.; Suzuki, T.; Kohori, A.; Itoh, H.; Yoshida, M.; Kinosita, K., Jr. *Science* **2008**, *319*, 955–958.
(25) Hossain, M. D.; Furuike, S.; Maki, Y.; Adachi, K.; Suzuki, T.; Kohori, A.; Itoh, H.; Yoshida, M.; Kinosita, K., Jr. *Biophys. J.* **2008**, *95*, 4837–4844.
(26) Yagi, H.; Tsujimoto, T.; Yamazaki, T.; Yoshida, M.; Akutsu, H. *J. Am. Chem. Soc.* **2004**, *126*, 16632–16638.
(27) Yagi, H.; Kajiwara, N.; Iwabuchi, T.; Izumi, K.; Yoshida, M.; Akutsu, H. *J. Biol. Chem.* **2009**, *284*, 2374–2382.
(28) Masaike, T.; Mitome, N.; Noji, H.; Muneyuki, E.; Yasuda, R.; Kinosita, K., Jr.; Yoshida, M. *J. Exp. Biol.* **2000**, *203*, 1–8.
(29) Ito, Y.; Ikeguchi, M. *Chem. Phys. Lett.* **2010**, *490*, 80–83.
(30) Arora, K.; Brooks, C. L., III. *Proc. Natl. Acad. Sci. U.S.A.* **2007**, *104*, 18496–18501.
(31) Arora, K.; Brooks, C. L., III. *J. Am. Chem. Soc.* **2009**, *131*, 5642–5647.
(32) Jonsson, H.; Mills, G.; Jacobsen, K. W. . In *Classical and Quantum Dynamics in Condensed Phase Simulations*; Berne, B. J., Cicotti, G., Coker, D. F., Eds.; World Scientific: Rivers Edge, NJ, 1998; pp 385−404.
(33) Chu, J. W.; Trout, B. L.; Brooks, B. R. *J. Chem. Phys.* **2003**, *119*, 12708–12717.
(34) Torrie, G. M.; Valleau, J. P. *Chem. Phys. Lett.* **1974**, *28*, 578–581.
(35) Kirkwood, J. G. *J. Chem. Phys.* **1935**, *3*, 300–313.
(36) Banavali, N. K.; Roux, B. *J. Am. Chem. Soc.* **2005**, *127*, 6866–6876.
(37) Banavali, N. K.; Roux, B. *Structure* **2005**, *13*, 1715–1723.
(38) Brooks, B. R.; Bruccoleri, R. E.; Olafson, B. D.; States, D. J.; Swaminathan, S.; Karplus, M. *J. Comput. Chem.* **1983**, *4*, 187–217.
(39) Kumar, S.; Bouzida, D.; Swendsen, R. H.; Kollman, P. A.; Rosenberg, J. M. *J. Comput. Chem.* **1992**, *13*, 1011–1021.
(40) Bowler, M. W.; Montgomery, M. G.; Leslie, A. G. W.; Walker, J. E. *J. Biol. Chem.* **2007**, *282*, 14238–14242.
(41) Ikeguchi, M. *J. Comput. Chem.* **2004**, *25*, 529–541.
(42) MacKerell, A. D., Jr.; et al. *J. Phys. Chem. B* **1998**, *102*, 3586–3616.
(43) MacKerell, A. D., Jr.; Feig, M.; Brooks, C. L., III. *J. Comput. Chem.* **2004**, *25*, 1400–1415.
(44) Jorgensen, W. L.; Chandrasekhar, J.; Madura, J. D.; Impey, R. W.; Klein, M. L. *J. Chem. Phys.* **1983**, *79*, 926–935.
(45) Essmann, U.; Perera, L.; Berkowitz, M. L.; Darden, T.; Lee, H.; Pedersen, L. G. *J. Chem. Phys.* **1995**, *103*, 8577–8593.
(46) Amano, T.; Tozawa, K.; Yoshida, M.; Murakami, H. *FEBS Lett.* **1994**, *348*, 93–98.
(47) Löbau, S.; Weber, J.; Wilke-Mounts, S.; Senior, A. E. *J. Biol. Chem.* **1997**, *272*, 3648–3656.
(48) Ariga, T.; Muneyuki, E.; Yoshida, M. *Nat. Struct. Mol. Biol.* **2007**, *14*, 841–846.
(49) Nadanaciva, S.; Weber, J.; Senior, A. E. *Biochemistry* **1999**, *38*, 7670–7677.
(50) Dittrich, M.; Hayashi, S.; Schulten, K. *Biophys. J.* **2004**, *87*, 2954–2967.
(51) Ahmad, Z; Senior, A. E. *J. Biol. Chem.* **2004**, *279*, 31505–31513.
(52) Kobayashi, M.; Akutsu, H.; Suzuki, T.; Yoshida, M.; Yagi, H. *J. Mol. Biol.* **2010**, *398*, 189–199.
(53) Hayward, S. *Protein Sci.* **2001**, *10*, 2219–2227.
(54) Daggett, V. *Acc. Chem. Res.* **2006**, *39*, 594–602.
(55) Armen, R. S.; DeMarco, M. L.; Alonso, D. O.; Daggett, V. *Proc. Natl. Acad. Sci. U.S.A.* **2004**, *101*, 11622–11627.
(56) Shimabukuro, K.; Muneyuki, E.; Yoshida, M. *Biophys. J.* **2006**, *90*, 1028–1032.
(57) Enoki, S.; Watanabe, R.; Iino, R.; Noji, H. *J. Biol. Chem.* **2009**, *284*, 23169–23176.
(58) Yoshidome, T.; Kinoshita, M.; Hirota, S.; Baden, N.; Terazima, M. *J. Chem. Phys.* **2008**, *128*, 225104(1−9).
(59) Kauzmann, W. *Adv. Protein Chem.* **1959**, *14*, 1–63.
(60) Gerstman, B. S.; Chapagain, P. P. *J. Chem. Phys.* **2005**, *123*, 054901(1−6).
(61) Foulkes-Murzycki, J. E.; Scott, W. R.; Schiffer, C. A. *Structure* **2007**, *15*, 225–233.
(62) Weber, J.; Wilke-Mounts, S.; Lee, R. S.; Grell, E.; Senior, A. E. *J. Biol. Chem.* **1993**, *268*, 20126–20133.
(63) Watanabe, R.; Iino, R.; Shimabukuro, K.; Yoshida, M.; Noji, H. *EMBO Rep.* **2008**, *9*, 84–90.
(64) Masaike, T.; Koyama-Horibe, F.; Oiwa, K.; Yoshida, M.; Nishizaka, T. *Nat. Struct. Mol. Biol.* **2008**, *15*, 1326–1333.
(65) Menz, R. I.; Walker, J. E.; Leslie, A. G. *Cell* **2001**, *106*, 331–341.
(66) Hirono-Hara, Y.; Noji, H.; Nishiura, M.; Muneyuki, E.; Hara, K. Y.; Yasuda, R.; Kinosita, K., Jr.; Yoshida, M. *Proc. Natl. Acad. Sci. U.S.A.* **2001**, *98*, 13649–13654.